

# A continuum self organized criticality model of turbulent heat transport in tokamaks

Varun Tangri, Amita Das, Predhiman Kaw and Raghvendra Singh  
Institute for Plasma Research, Bhat, Gandhinagar, 382428, India

**Abstract.** Based on the now well known and experimentally observed critical gradient length ( $R/L_{Te} = RT/\nabla T$ ) in tokamaks, we present a continuum one dimensional model for explaining self organized heat transport in tokamaks. Key parameters of this model include a novel hysteresis parameter which ensures that the switch of heat transport coefficient  $\chi$  upwards and downwards takes place at two different values of  $R/L_{Te}$ . Extensive numerical simulations of this model reproduce many features of present day tokamaks such as submarginal temperature profiles, intermittent transport events,  $1/f$  scaling of the frequency spectra, propagating fronts etc. This model utilises a minimal set of phenomenological parameters, which may be determined from experiments and/or simulations. Analytical and physical understanding of the observed features has also been attempted.

## 1 Introduction

Recent experimental work on turbulence driven heat transport in tokamaks has revealed many features which are consistent with a self - organized criticality (SOC)[1] model of transport[2]. Notable among these features[*e.g.* for electron heat transport] are (i) observation of a threshold [3](typically sub - marginal) temperature profile with a strong tendency towards ‘profile consistency’ [4](*i.e.* relative insensitivity of the measured profile shape to the radial distribution of heat source); (ii) large scale intermittent transport events (as revealed by electron cyclotron emission measurements) exhibiting long time auto - correlations[7]; (iii) characteristic frequency spectra showing scaling behavior,  $f^{-\alpha}$  with  $\alpha \sim 1$  [6]; (iv) observation of non - diffusive radial propagation of fronts associated with avalanche events with speeds of order few hundred meters/sec[5] etc. Most of the features discussed above are generic for turbulent transport in toroidal devices and have also been observed in studies of core ion transport, edge heat transport, flux driven scrape off layer transport[7]-[13] *etc.* Full scale three dimensional gyrofluid and gyrokinetic simulations have also been carried out and reveal a complex and rich interplay, for example between the basic temperature gradient driven instability (*e.g.* ETG) and related modulational instabilities leading to generation of zonal flows, streamers *etc*[14]. Such simulations often reproduce many of the features of the transport, observed in experiments[15]. However, they are typically so complex, that one does not get a good idea about the most important physics which is responsible for the observed phenomena. At the other end of the spectrum are highly oversimplified, discrete, cellular automaton type models which also reproduce many of the observed features[16]; they, however, give us no insight into the relevant physics issues and appear to be highly contrived.

We follow a middle path considering the following fact: Analytical calculations of electron heat transport [] have shown that when  $\eta_e = d \ln T / d \ln n$  exceeds a critical value, short scale, fast growing electrostatic modes generally known as the electron temperature

gradient modes (ETG) are excited. These modes leave the ion transport unaffected and enhance the electron thermal conductivity  $\chi$ . Investigated by several authors[], linear and nonlinear theories of this mode generally give  $\chi_{ETG}$  of the following form[]:

$$\chi_{ETG} = \chi_{min} + \chi_{max} G\left(\frac{R}{L_{Te}} - \left(\frac{R}{L_{Te}}\right)_c\right) \quad (1)$$

where  $G$  is the heaviside step function  $G(x) = 1 \forall x > 0$  and  $G(x) = 0 \forall x \leq 0$ ;  $L_{Te} = T/\nabla T$  is the gradient length and  $R$  is the major radius.  $\chi_{min}$  is the transport coefficient in absence of temperature gradient turbulence and  $\chi_{max}$  is the transport coefficient associated with saturated ETG turbulence. Such a form for  $\chi$  finds support from experiments and simulations[].

Using the above idea, we propose the application of a one - dimensional continuum model of driven dissipative systems, to the electron thermal transport problem in tokamaks. This simple model set of equations is able to reproduce all the observed features of the transport discussed above in terms of a few phenomenological parameters. We offer an analytic description of some of the observed phenomena and also discuss how the key phenomenological parameters may be obtained from experiments and/or detailed 3 - dim computer simulations.

The remaining part of this article is organized as follows: Sec II describes the basic model used whose results are presented in Sec III. The final we conclusions are discussed in Sec IV.

## 2 Basic Model

We adapt a model introduced by Lu [17] for the description of SOC behaviour in solar flares to heat transport in tokamaks. Such a model has also been applied to the magnetic substorm problem recently by Klimas et al[18]. It consists of a set of two coupled equations - a 1-d radial transport equation with sources and a nonlinear relaxation equation for the turbulence driven transport coefficient  $\chi$ :-

$$\frac{\partial T}{\partial t} = \frac{\partial}{\partial x} \left( \chi \frac{\partial T}{\partial x} \right) + S(x, t) \quad (2)$$

$$\frac{\partial \chi}{\partial t} + \chi = Q(x, t) \quad (3)$$

where we have used normalized variables  $T = \bar{T}/T_0$ ,  $x = \bar{x}/x_0$ ,  $t = \bar{t}/\tau$ ,  $\chi = \bar{\chi}\tau/x_0^2$ ,  $S = P\tau/(3nT_0/2)$ .  $P$  is the input power density which determines the source  $S$ .  $n$  is the plasma density,  $x_0$ ,  $T_0$  are normalizing variables,  $\tau$  is the natural nonlinear relaxation time of the  $\chi$  equation.

The source function  $Q$  for  $\chi$  is a double valued function switching between two values  $\chi_{max}$  and  $\chi_{min}$  and has hysteresis. For the problem at hand, we have studied two special forms for the function  $Q$ :

$$Q = \begin{cases} \chi_{max} & \text{if } \frac{dT}{dX} > k \\ \chi_{min} & \text{if } \frac{dT}{dX} < \beta k \end{cases} \quad Q = \begin{cases} \chi_{max} & \text{if } \frac{1}{T} \frac{dT}{dX} > k \\ \chi_{min} & \text{if } \frac{1}{T} \frac{dT}{dX} < \beta k \end{cases} \quad (4)$$

Thus  $Q$  changes from  $\chi_{min}$  to  $\chi_{max}$  when  $\nabla T$  (or  $\frac{1}{T}\nabla T$ ) exceeds a critical value  $k$  but switches back from  $\chi_{max}$  to  $\chi_{min}$  only if  $\nabla T$  (or  $\frac{1}{T}\nabla T$ ) is less than  $\beta k$ ;  $\beta$  is the hysteresis

parameter and takes values less than 1. The presence of hysteresis (i.e.  $\beta \neq 1$ ) in the source function  $Q$  is crucial for the depiction of SOC characteristics; hysteresis is related to the physical fact that once the turbulence is excited it may be possible to sustain it even when  $\nabla T$  goes below the linear instability threshold.

In the next section, we present results of our simulations for  $\beta \neq 1$ . Sec 3.1 discusses results using Eq. 4(a) and Sec 3.2 discusses those using 4(b).

### 3 Results

We have numerically solved Eq.(2) and Eq.(3) by finite differencing in space and the time advancement is carried out by the gear method. We present results for the case when the source function is of the form  $S(x) = S_0 \sin(\pi x/2L)$ , however runs with other forms indicate that any special form for  $S(x)$  is not important. The box size has been fixed at  $L = 20$  and the value of the critical slope parameter and the hysteresis parameter respectively are  $k = 0.04$  and  $\beta = 0.9$ .  $\chi_{max}$  and  $\chi_{min}$  are chosen to be 2 and 0.2, respectively and  $S_0$  is chosen in the range  $10^{-3}$  to  $10^{-2}$ . As explained later, these dimensionless values correspond to typical numbers characteristic of tokamaks like JET, TORE-SUPRA and D-III D.

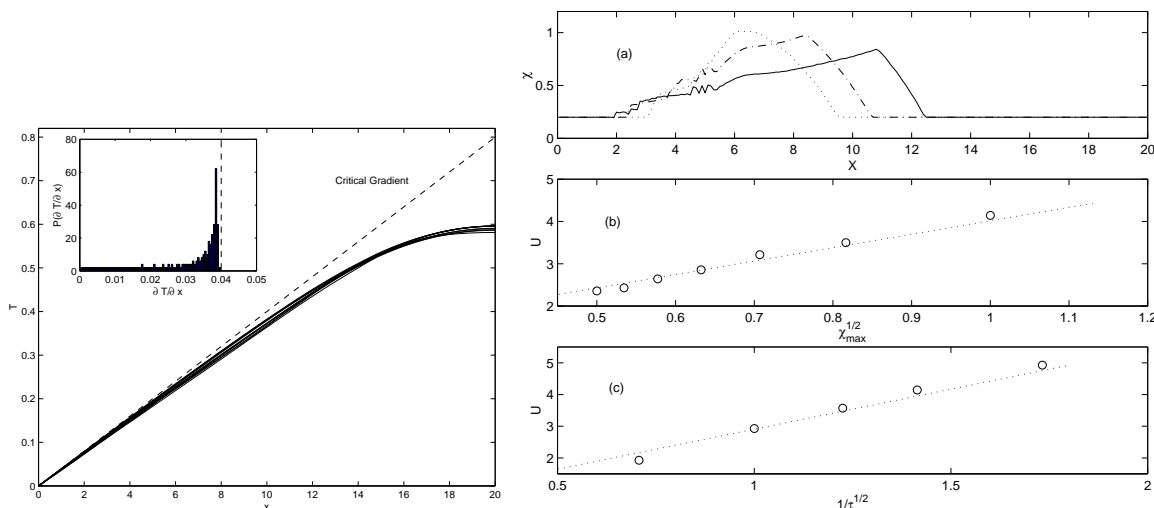


FIG. 1. Subcritical profiles superimposed for various times. The inset shows the probability distribution function of the temperature gradient  $\partial T/\partial x$  (a) Propagation of fronts. The variation of velocity of fronts  $U$  with (b) varying  $\chi_{max}$ , (c) varying  $1/\tau^{1/2}$

#### 3.1 Critical gradient based model

The plot in Fig.1 (left side) obtained numerically shows clearly that profile of  $T$  (after an initial transient) approaches a state where the  $\nabla T$  is below the critical slope at nearly all positions. In our numerical experiments we included (1)nearly linear  $T(x) \sim kx$ , (2) random  $T(x) > 0$ , initial profiles. In each of these cases, the instantaneous  $T$  profile very rapidly approaches a subcritical state. This result is consistent with the experimental observation of sub - marginal thresholds. Furthermore, in time, a complex sequence of avalanches carrying the flux of  $T$  through the system are observed as required for the SOC state. The detailed results exhibited by this model can be summarized as follows: (i) the

simulations show (Fig.1a) propagating front like structures in the gradient of  $T$  field (as well as in the diffusivity  $\chi$ ). These fronts propagate with a constant velocity  $\bar{U}$ . (ii) The velocity  $\bar{U}$  is found to scale as  $\sqrt{\bar{\chi}_{max}/\tau}$  (Fig.1b,c). (iii) The total energy of the system defined by  $E(t) = \int dx T^2(x, t)$  (which is like the thermal energy  $nT$  if  $n(x)$  and  $T(x)$  are taken to be identical functions for simplicity) shows quasiperiodic behavior with a steady linear rise with time (loading) and a sudden crash (unloading) displaying a saw tooth form (Fig2a). (iv) The amplitude  $\Delta E = E_{max} - E_{min}$  and frequency  $\nu$  of such saw tooth events are in general of statistical nature. However, their mean values are observed to depend on the parameters  $\chi_{min}$  and the source strength  $S_0$ . (v) The value of  $\Delta E$  and  $\nu$  also depend on the hysteresis parameter  $\beta$ . The mean value  $\langle \Delta E \rangle$  scales linearly with  $(1 - \beta^2)$  (Fig.2b). We note that the model makes predictions which are in conformity with special features of electron thermal transport in tokamaks. Thus observations (i) and (ii) are related to the radial propagation of avalanche fronts across a discharge and observations (iii) - (iv) show the intermittent bursty nature of the transport (Fig.2c). While the observations

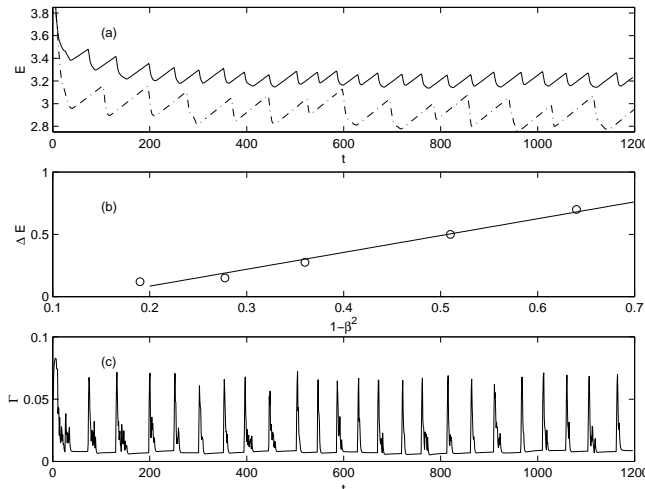


FIG. 2. Loading Unloading cycle: (a) Plot of  $E$  vs time (b) Mean Cycle Amplitude  $\Delta E$  vs  $1 - \beta^2$  (c) Evolution of Flux

(i), (iii) and (iv) above are similar to those obtained earlier by Klimas *et al.*[18], for the substorm problem, (ii) and (v) are new results and have been obtained by us after extensive numerical simulations. We now provide a simple theoretical interpretation of the above results; such an interpretation has not been attempted in earlier work.

Our simulations show propagating spatio temporal front structures in  $\partial T/\partial x$  (and so also in  $\chi$ ). Well within the boundaries of  $x$  space these fronts typically move with a constant velocity. We observe that the propagation speed depends on the parameters  $\chi_{max}$ ,  $\beta$  and  $\tau$  with the scaling of  $\bar{U} \propto \sqrt{\bar{\chi}_{max}/\tau}$  as shown in Fig.1. Such a scaling can be understood from the following simplified analysis. The front structure in the diffusion coefficient arises due to the switching of  $Q$  from  $\chi_{min}$  to  $\chi_{max}$ , at locations where the local slope exceeds the critical value  $k$ . The subsequent evolution of the diffusivity with time (so long as  $Q$  remains at  $\chi_{max}$ ) as governed by Eq.(3) is given by the following expression

$$\chi(t) = \chi_{max} \{1 - \exp(-t)\} + \chi_{min} \exp(-t) \quad (5)$$

For  $\chi_{min} \ll \chi_{max}$  (as indeed is the case) and for a time  $t \ll 1$  we can approximate the expression for  $\chi$  as  $\chi = \chi_{max} t$ . We may now write the diffusion equation as  $\partial T/\partial \eta = \partial^2 T/\partial x^2$  where  $\eta = \chi_{max} t^2/2$ ; exact solution shows diffusion in  $x - \eta$  variables,  $x^2 \approx \eta \approx$

$\chi_{max}t^2/2$  giving a front propagation speed in dimensional variables as  $\bar{U} = \frac{\bar{x}}{t} \approx \sqrt{\frac{\bar{\chi}_{max}}{2\tau}}$ . Figures (1b,c) give plots illustrating this scaling as observed in the numerical simulations.

The quasiperiodic oscillations of energy (Fig 2a) having a saw tooth character in time, signifies a slow building up of the temperature profile from  $\beta kx$  towards  $kx$  by the source function followed by a sudden crash. The maximum amount of energy that can be released by the system in a crash can be estimated from the difference of the energies of the two states. The state  $T = \beta kx$ , thus defines the minimum energy and is given by  $E_{min} = \int T^2 dx = \beta^2 k^2 \int x^2 dx = \beta^2 k^2 L^3/3$ . On the other hand the maximum energy that can be retained by the system so that  $T = kx$  is given by  $E_{max} = \int T^2 dx = k^2 \int x^2 dx = k^2 L^3/3$ . The difference  $\Delta E = E_{max} - E_{min} = (1 - \beta^2)E_{max} = (1 - \beta^2)k^2 \frac{L^3}{3}$  gives the maximum amplitude of  $\Delta E$  in the growth and decay cycle that the system can exhibit. The observed amplitudes, in general are typically lower than the above estimate because  $L$ , the box size should be replaced by  $l$  representing the typical avalanche size in above expression. Thus the average energy release in the avalanches is  $\langle \Delta E \rangle = (1 - \beta^2)k^2 \bar{l}^3/3$ , confirming the observed scaling with  $\beta$  which can be seen from the plot of Fig.2b and mentioned earlier in the point (v) of the summary of results.

The parameter  $\chi_{min}$  essentially determines the spatial correlation length  $l_c$  for  $T$  [note that for  $\chi_{min} = 0$  during the growth phase, Eq.(2) turns into an ordinary differential i.e.  $l_c = 0$ ]. As  $\chi_{min}$  is increased it correlates  $T$  over disparate spatial regions by diffusion. Thus a high value of  $\chi_{min}$  might seem desirable. However, the dissipation due to  $\chi_{min}$  should not exceed input via source term leading to a damped final state. Hence an optimum  $\chi_{min}$  can be estimated by the critical balance condition  $\chi_{min} \partial^2 T / \partial x^2 = -S_0 \sin(\pi x/2L)$  which implies that  $T = T_0 \sin(\pi x/2L)$  where  $\chi_{min}(\pi/2L)^2 T_0 = S_0$ . The value of  $T_0$  can be estimated by requiring that maximum value of the slope does not exceed the critical value of  $k$  at any location; thus  $(\partial T / \partial x)_{max} = (T_0 \pi/2L) \leq k = 0.04$ . For our simulation we have  $L = 20$ ,  $S_0 = 3 \times 10^{-4}$  implying that  $\chi_{min} = 0.1$  for best avalanches.

We now discuss in somewhat more detail the implications of the results of this model for the electron thermal transport in tokamaks. First, we look at some numbers. If we take  $x_0 = 2.5$  cms,  $T_0 = 10$  KeV,  $\tau \approx 10^{-4}$  secs,  $\bar{\chi}_{max} \approx 10^5 cm^2/sec$ ,  $n \approx 10^{13} \times 5 cm^{-3}$ ,  $P \approx 1 MW/m^3$ , we are considering a 50cm radius plasma with a peak temperature of about 8 keV with  $\approx 10 MW$  of input power which is like the plasma in Tore - Supra experiment; this choice gives us dimensionless parameters  $L = 20$ ,  $S = 10^{-3}$ ,  $\chi_{max} \approx 2$  as shown in our sample simulation. Experiments like JET and D-III D also give a similar parameter range for the simulations. The choice of  $\tau$  and  $\bar{\chi}_{max}$  needs comment.  $\tau$  is a nonlinear relaxation time for the ETG turbulence which describes the time taken by  $\chi$  to stabilize at  $\chi_{max}$  after  $\nabla T$  crosses the critical value  $k$ . This involves saturation of the ETG turbulence, growth of streamer like modulational instabilities (since they dominate the ETG transport) and their saturation by Kelvin - Helmholtz secondary instabilities. Estimate of  $\tau$  can be made from large scale simulations and/or from experiments; they give a value of order  $\tau \sim 10^3 L_t / V_{th} \approx 100 \mu secs$  where  $V_{th}/L_T$  is the typical ETG growth rate.  $\bar{\chi}_{max}$  is the upper limit to which  $\bar{\chi}$  can rise; it typically never reaches there because avalanches strike. Thus  $\bar{\chi}_{max} \sim 3 \bar{\chi}_{meas}$  and is taken as  $\sim 10^5 cm^2/sec$ . The choice of hysteresis parameter  $\beta = 0.9$  is somewhat ad - hoc; its main effect, however, is to limit the size of the fluctuations in energy.

### 3.2 Critical gradient length based model

In this section, we shall present the results from the  $\nabla T/T$  model described in eq (4). Following parameters have been chosen for this simulation:  $k=0.25, \beta = 0.9, \tau=1, \chi_{max} = 12, \chi_{min} = 0.2, S_o = 0.1$  and  $L = 20$ . This implies  $T_o=0.1\text{KeV}$  and  $P=1.2\text{MW}$ . The boundary conditions used in this model are:  $\frac{\partial T}{\partial x}(x = L)=0$  and  $\chi \frac{\partial T}{\partial x}(x = 0) = \int S(x)dx$ . As shown in fig 3(a), the PDF of  $\nabla T/T$  indicates submarginality - the most probable value of  $\nabla T/T$  lies below  $k$ . Dashed line here indicates the critical value  $k$ . The observation that  $1/L_{Te}$  mostly lies below this line reinforces the above fact. In Figure 4(a), a time series of flux,  $\Gamma$  is shown. We define  $\Gamma(x, t) = \chi(x, t)\partial T/\partial x$ . The power spectra obtained from a the

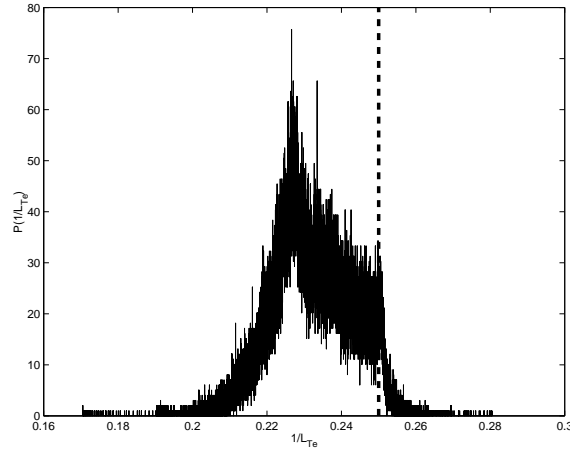


FIG. 3. The probability distribution of the  $1/L_{Te} = \nabla T/T$  from a time series accumulated at a point.

time series of flux (Figure 4b) indicates a  $1/f^\alpha$  with  $\alpha \sim 1$  type of power spectrum. Such a power spectrum is a signature of self organized criticality. Experimental observations on various tokamaks have reported similar spectra [eg see Politzer et al []]. Along with

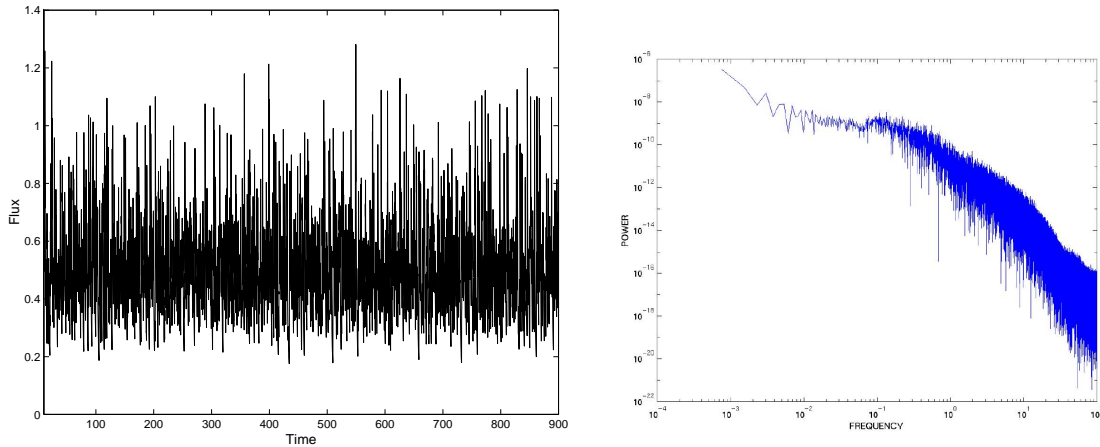


FIG. 4. a) Time evolution of Flux at b) Power spectrum of flux  $\Gamma$

a power law tail, Hurst parameter  $H$ , also characterizes such events (politzer et al[] and references therein). This parameter characterizes the behaviour of the autocorrelation at large lag times. For a long time correlation,  $1/2 < H < 1$ , while  $0 < H < 1/2$  indicates anticorrelation. We have made measurement of Hurst parameter from our simulation data by the method of R/S statistics (Figure 5a). The simulation data presented here gives

$H = 0.94$ . Having  $H$  so close to one indicates that events are occurring on all timescales, down to the numerical the time step. The value obtained by us is somewhat larger than that obtained from actual experiments (Politzer et al (POP)). To further analyze our

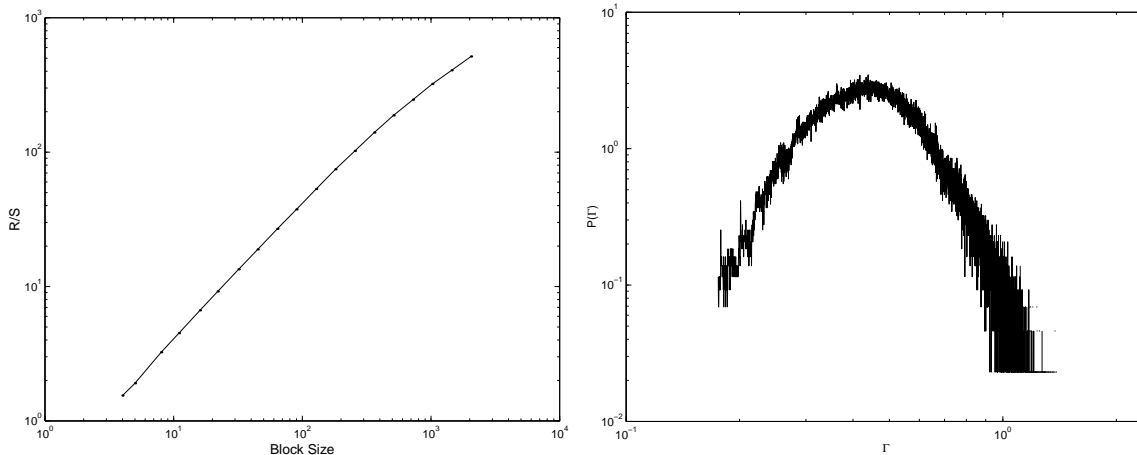


FIG. 5. a) Hurst parameter from a time series of flux. b) Probability distribution function  $P(\Gamma_T)$

studies of the statistical properties of Flux as obtained from our system of equations, we have also obtained the probability distribution function of flux. We define the probability distribution function  $P(\Gamma_T) = N_{\Gamma_T}/NW$  where  $N_{\Gamma_T}$  is the number of data values that fall between  $\Gamma_T$  and  $\Gamma_T + W$ ,  $W$  is a narrow interval starting at  $\Gamma_T$  and  $N$  is the total number of data values. Figure 5b shows the probability distribution function (PDF) of a flux time series accumulated at a point near the edge.

## 4 Conclusions

Using a 1-d model has reproduced many observed features of electron thermal transport. These include: (i) sub - marginal temperature profiles (ii) profile resilience (iii) intermittent large scale transport events (iv) power spectrum (v) radially propagating fronts with speeds of order  $(\bar{\chi}_{max}/2\tau)^{1/2} \sim 200m/sec$ . (vi) measurements of the PDF of flux and and the hurst parameter indicate occurrence of avalanche events on all time scales.

It would be interesting to to verify the physics described here and to determine the phenomenological parameters introduced. There is already abundant experimental data on critical threshold gradient length  $L_{Te}$ . Active experiments with localized heat sources like ECRH could be carried out to measure  $\chi_{max}$ ,  $\chi_{min}$ , the relaxation time  $\tau$ , the hysteresis parameter  $\beta$  etc. Similarly, simulations and analytical theory could be used to understand the magnitudes of these phenomenological parameters and would thus elucidate the physics of the phenomena a little better.

Finally, we emphasize that the paradigm introduced here for electron thermal transport is much more general and may be applicable to a number of observations in magnetically confined plasmas (with appropriate modifications) such as ELMS, flux driven transport in scrape - off - layers, ion thermal transport and particle transport in core regions etc. It may also be useful to extend these 1-d models to situations involving coupled transport equations in density, temperatures, currents, etc.

# References

- [1] BAK P., TANG C., WIESENFELD K., “self organized criticality: An explanation of  $1/f$  noise”, Phys. Rev. Lett, **59**, 381 (1987); Phys. Rev. A **38**, 364 (1988).
- [2] DIAMOND P. H., HAHM T. S. Phys. Plasmas **2** 3640 (1995)
- [3] HOANG G. T. *et al.*, “Experimental determination of critical threshold in electron transport on Tore Supra” Phys. Rev. Lett. **87** 125001 (2001).
- [4] RYTER F. *et al.*, “ Experimental evidence for Gradient Length driven Electron transport in Tokamaks” Phys. Rev. Lett. **86** 2325 (2001); OHYABU N., *et al.*, “ Edge transport barriers and  $T_e$  profile stiffness in LHD” Plasma Phys. Control. Fusion **44** A211-A216 (2002).
- [5] POLITZER P. A., Phys. Rev. Lett 1195 (2000).
- [6] POLITZER P. A. *et al.*, Phys Plasmas **9** 1962 (2002).
- [7] CARRERAS B. A., *et al.*, “ Long range time correlations in plasma edge turbulence” Phys. Rev. Lett **80** 4438 (1998).
- [8] PEDROSA M. A., *et al.*, “Empirical similarity of frequency spectra of the edge plasma fluctuations in toroidal magnetic-confinement systems”, Phys. Rev. Lett. **82**, 3621 (1999).
- [9] SARAZIN Y. and GHENDRIH Ph., Phys Plasmas **5** 4214 (1998).
- [10] GARBET X., WALTZ R. E., “Flux driven ion turbulence” Phys Plasmas **5** 2836 (1998).
- [11] ANTAR G. Y. *et al.*, “ Turbulent intermittency and burst properties in tokamak scrape off layer”, Phys Plasmas **8** 1612 (2001).
- [12] JHA R. *et al.*, “Intermittency in edge turbulence “, Phys Rev Lett. **69** 1375 (1992).
- [13] BEYER P., *et al.*, “Non diffusive transport in tokamaks: Three dimensional structure of bursts and the role of zonal flows”, Phys. Rev. Lett. **85** 4892 (2000).
- [14] DORLAND W., JENKO F., KOTSCHENREUTHER M., ROGERS B. N. Phys. “Electron temperature gradient Turbulence”, Rev. Lett. **85** 5579 (2000).
- [15] CARRERAS B. A. *et al.*, “A model self realization of self organized criticality for plasma confinement”, Phys Plasmas **3** 2903 (1996).
- [16] NEWMAN D. E., *et al.*, Phys Plasmas **3** 1858 (1996).
- [17] LU E. T., Phys. Rev. Lett, **74**, 2511 (1995).
- [18] KLIMAS A. J., *et al* J. Geophys. Res, **105** A8, 18765 (2000).